Biochemical Pharmacology 77 (2009) 1374–1382

Contents lists available at ScienceDirect

Biochemical Pharmacology

journal homepage: www.elsevier.com/locate/biochempharm

# Identification of transmembrane domain 6 & 7 residues that contribute to the binding pocket of the urotensin II receptor

Brian J. Holleran, Ivana Domazet, Marie-Eve Beaulieu, Li Ping Yan, Gaétan Guillemette, Pierre Lavigne, Emanuel Escher, Richard Leduc *

*Department of Pharmacology, Faculty of Medicine and Health Sciences, Université de Sherbrooke, Sherbrooke, Quebec, Canada J1H 5N4*

ARTICLE INFO

*Article history:*
Received 18 November 2008
Accepted 21 January 2009

*Keywords:*
Urotensin II
Urotensin II receptor
GPCR
Substituted-cysteine accessibility method
Ligand-binding pocket

ABSTRACT

Urotensin II (U-II), a cyclic undecapeptide, is the natural ligand of the urotensin II (UT) receptor, a G protein-coupled receptor. In the present study, we used the substituted-cysteine accessibility method to identify specific residues in transmembrane domains (TMDs) six and seven of the rat urotensin II receptor (rUT) that contribute to the formation of the binding pocket of the receptor. Each residue in the R256$^{(6.32)}$-Q283$^{(6.59)}$ fragment of TMD6 and the A295$^{(7.31)}$-T321$^{(7.57)}$ fragment of TMD7 was mutated, individually, to a cysteine. The resulting mutants were expressed in COS-7 cells, which were subsequently treated with the positively charged methanethiosulfonate-ethylammonium (MTSEA) or the negatively charged methanethiosulfonate-ethylsulfonate (MTSES) sulfhydryl-specific alkylating agents. MTSEA treatment resulted in a significant reduction in the binding of TMD6 mutants F268C$^{(6.44)}$ and W278C$^{(6.54)}$ and TMD7 mutants L298C$^{(7.34)}$, T302C$^{(7.38)}$, and T303C$^{(7.39)}$ to $^{125}$I-U-II. MTSES treatment resulted in a significant reduction in the binding of two additional mutants, namely L282C$^{(6.58)}$ in TMD6 and Y300C$^{(7.36)}$ in TMD7. These results suggest that specific residues orient themselves within the water-accessible binding pocket of the rUT receptor. This approach, which allowed us to identify key determinants in TMD6 and TMD7 that contribute to the UT receptor binding pocket, enabled us to further refine our homology-based model of how U-II interacts with its cognate receptor.



## 1. Introduction

Urotensin II (ETPDCFWKYCV, U-II) is a cyclic undecapeptide with vasoactive, proliferative, neuronal, and chemotactic properties. U-II is the endogenous ligand of the urotensin II (UT) receptor, which is considered a pharmacological target for treating cardiovascular diseases (hypertension, heart failure, cardiac fibrosis, and hypertrophy), atherosclerosis, liver diseases, and diabetes [14,15,26,28]. U-II was originally isolated from the urophysis of teleost fish [30], and the cDNA encoding its precursor has been identified in many species [9,10]. The UT receptor is a member of family 'A' of the larger G protein-coupled receptor (GPCR) superfamily [2]. Many features associated with this family such as a short N-terminus, a highly conserved residue in each transmembrane domain (TMD), a D/ERY motif in the second intracellular loop, a CW/FxP 'toggle switch' motif [32] in TMD6, a NPxxY motif in TMD7, and potential serine/threonine phosphorylation sites in the cytoplasmic tail [31] are found in the UT receptor.

The molecular mechanisms by which agonists bind to and activate GPCRs through conformational changes remain obscure. Although for many years, the only available structural model was rhodopsin [27], the structures of other GPCRs such as the β2 adrenergic [7], β1 adrenergic [34], opsin [29], and $A_{2A}$ adenosine receptors [19] have recently been determined. These studies have enabled us to better understand how diffusible ligands can recognize and bind to GPCRs, and how TMDs are involved in this process. For instance, the $A_{2A}$ adenosine structure clearly shows how both TMD6 and TMD7 play a role in the formation of the receptor's binding pocket [19].

Despite these major advances, many questions remain regarding the dynamics by which conformers shift from the ground state to an active state. A variety of biophysical and biochemical approaches are needed to help address these issues. The substituted-cysteine accessibility method (SCAM) [1,21,22] is an ingenious approach for systematically identifying TMD residues that contribute to the binding-site pocket of GPCRs. Consecutive residues within TMDs are mutated to cysteine, one at a time, and the mutant receptors are expressed in heterologous cells. If ligand

* Corresponding author. Tel.: +1 819 564 5413; fax: +1 819 564 5400.
*E-mail address:* Richard.Leduc@USherbrooke.ca (R. Leduc).

0006-2952/$ – see front matter © 2009 Elsevier Inc. All rights reserved.
doi:10.1016/j.bcp.2009.01.013

binding to a cysteine-substituted mutant is unchanged compared to wild-type receptor, it is assumed that the structure of the mutant receptor, especially around the binding site, is similar to that of the wild-type receptor and that the substituted cysteine lies in a orientation similar to that of the residue of the wild-type receptor. In TMDs, the sulfhydryls of cysteines oriented toward the aqueous binding-site pocket should react more quickly with charged sulfhydryl reagents like methanethiosulfonate-ethylammonium (MTSEA) and methanethiosulfonate-ethylsulfonate (MTSES) than the sulfhydryls of cysteines that face the interior of the protein or the lipid bilayer. Two criteria are used to determine whether engineered cysteines are positioned at the surface of the binding-site pocket: (i) the reaction with the MTS reagent alters binding irreversibly and (ii) the reaction is retarded by the presence of the ligand. This approach has been used by us and others to identify residues that line the surface of GPCR binding-site pockets [3,17,20,24,25,36]. Here, we report the application of SCAM to probe TMD6 and TMD7 of the rat UT receptor.

## 2. Materials and methods

### 2.1. Materials

Bovine serum albumin (BSA) and bacitracin were from Sigma–Aldrich (Oakville, ON, Canada). FUGENE®-6 was from Roche Molecular Biochemicals (Mannheim, Germany). The sulfhydryl-specific alkylating reagents MTSEA ($CH_3SO_2$-$SCH_2CH_2NH_3^+$) and MTSES ($CH_3SO_2$-$SCH_2CH_2SO_3^-$) were from Toronto Research Chemicals (Toronto, ON, Canada). The cDNA clone of the rUT receptor subcloned in the mammalian expression vector pcDNA3 was kindly provided by Dr. Brian O'Dowd (Department of Pharmacology, University of Toronto, Toronto, ON, Canada). DMEM (Dulbecco's modified Eagle's media), FBS (fetal bovine serum), and penicillin/streptomycin were from Gibco Life Technologies (Gaithersburg, MD, USA). Oligonucleotide primers were from IDT (Coralville, IA, USA). Human U-II was from Phoenix Pharmaceuticals (Belmont, CA, USA). $^{125}$I-U-II (specific activity 1000 Ci/mmol) was prepared using IODO-GEN® (1,3,4,6-tetrachloro-3α,6α-diphenyl-glycoluril; Pierce Chemical Co.,) as described by Fraker and Speck [16]. Briefly, 10 μl of a 1 mM peptide solution was incubated with 20 μg of IODO-GEN®, 80 μl of 100 mM borate buffer (pH 8.5), and 1 mCi of $Na^{125}I$ for 30 min at room temperature, and was then purified by HPLC on a C-18 column. The specific radioactivity of the labeled peptide was determined by self-displacement and saturation-binding analysis.

### 2.2. PCR mutagenesis

Mutant receptor cDNAs were constructed by oligonucleotide-directed mutagenesis (Expand High Fidelity PCR System; Roche Diagnostics) using rUT inserted into pcDNA3 (Invitrogen, Burlington, ON, Canada) as a template. A set of forward and reverse oligonucleotides were constructed to introduce cysteine mutations between R256$^{(6.32)}$ and Q283$^{(6.59)}$ for TMD6 and between A295$^{(7.31)}$ and Q283$^{(7.57)}$ for TMD7. PCR products were subcloned using KpnI and XbaI sites of pcDNA3 after digestion by the same restriction enzymes and the mutations were confirmed by nucleotide sequencing.

### 2.3. Cell culture and transfections

COS-7 cells were grown in Dulbecco's modified Eagle's medium (DMEM) containing 10% (v/v) fetal bovine serum, 100 IU/ml of penicillin, and 100 μg/ml of streptomycin at 37 °C. Semi-confluent cells (70%) in 100-mm-diameter Petri dishes were transfected using FUGENE®-6 as described by the manufacturer. Transfected cells were grown for 48 h before using them for the binding and SCAM assays.

### 2.4. Binding experiments

COS-7 cells were washed once with PBS and subjected to one freeze-thaw cycle. Broken cells were gently scraped into washing buffer (20 mM Tris–HCl, pH 7.4, 5 mM $MgCl_2$), centrifuged at 2500 × *g* for 15 min at 4 °C, and resuspended in binding buffer (20 mM Tris–HCl, pH 7.4, 5 mM $MgCl_2$, 0.1% BSA, 0.01% bacitracin). Saturation binding experiments were performed by incubating broken cells (20–40 μg of protein) for 1 h at room temperature with increasing concentrations of $^{125}$I-U-II (0.15–20 nM) in a final volume of 500 μl. Non-specific binding was determined in the presence of 1 μM unlabeled U-II. Bound radioactivity was separated from free ligand by filtration through GF/C filters presoaked for at least 1 h in binding buffer. Receptor-bound radioactivity was evaluated by γ-radiation counting. Results are presented as means ± SD. Binding data ($B_{max}$ and $K_d$) were analyzed with GraphPad Prism version 5.00 for Windows (GraphPad Software, San Diego, CA, USA) using a one-site binding hyperbola nonlinear regression analysis.

### 2.5. Treatment with MTS reagents

MTS treatments were performed according to the procedure of Javitch et al. [21], with minor modifications. Two days after transfection, the cells, which were grown in 12-well plates, were washed with PBS and incubated for 3 min at room temperature with freshly prepared MTSEA or MTSES at the desired concentrations (typically 0.5–6 mM) in a final volume of 200 μl. The reaction was stopped by washing the cells with ice-cold PBS. Intact cells were then incubated in binding medium (DMEM, 25 mM HEPES, pH 7.4, 0.1% BSA) containing 0.05 nM $^{125}$I-U-II for 120 min at room temperature. After washing with ice-cold PBS, cells were lysed with 0.1N NaOH and the radioactivity was evaluated by γ counting. The percentage of fractional binding inhibition was calculated as [1 − (specific binding after MTS-X treatment/specific binding without treatment)] × 100.

### 2.6. Protection against MTS reagents by U-II

Transfected cells grown in 12-well plates were washed once with PBS and incubated in the presence or absence of 100 nM U-II for 1 h at 16 °C (to avoid internalization of receptors). Cells were washed to remove excess ligand and were treated with the MTS reagent. Cells were washed three times with ice-cold PBS and once with an acidic buffer (150 mM NaCl, 50 mM acetic acid, pH 3.0) to dissociate bound ligand. They were then incubated for 3 h at 16 °C in binding medium (DMEM, 25 mM HEPES, pH 7.4, 0.1% BSA) containing 0.05 nM $^{125}$I-U-II. The percentage of protection was calculated as [(inhibition in the absence of U-II) − (inhibition in the presence of U-II)/(inhibition in the absence of U-II)] × 100.

### 2.7. Molecular modeling

All calculations were performed on a Silicon Graphics Octane2 workstation (Silicon Graphics Ins. Mountain View, CA, USA). The U-II and rUT receptor models were built using Insight II modules (Biopolymer, Homology, Discover; Accelrys, San Diego, CA, USA). The molecular model of U-II was constructed in a linear form using the Biopolymer module from Insight II. Subsequently, a disulfide bond was added between the residues in positions 5 and 10 of the ligand. The potential energy of the peptide was minimized for 500 steps with the steepest descents and a consistent valence force

field [11] using the Discover module. The minimized structure adopted the overall conformation previously reported for U-II [5]. A distance-dependent dielectric constant of 4 was used.

The theoretical structure of rUT (GenBank™ accession no. P49684) was generated by homology modeling based on the crystal structure of the β2 adrenergic receptor (Protein Data Bank: 2RH1), as described previously [8]. The resulting structure represents an inactive form of rUT with an overall configuration very similar to that of the β2 adrenergic receptor (1.38 Å RMSD between Cα of the transmembrane domains).

The U-II modeled structure was placed between the transmembrane domains of the rUT receptor, as suggested by the photolabeling results obtained with agonist ligands [4,18]. These results were used as distance restraints for the energy minimization of the U-II/rUT receptor complex. A first minimization of the complex between U-II and rUT receptor was performed using distance restraints (2 Å $< d <$ 7 Å) between the Sδ atoms of the photolabeled Met residues and the Cγ atom of the corresponding side chains on U-II. More specifically, residue $Glu^{1}$ was restrained to $Met^{288}$ [18], residue $Phe^{6}$ was restrained to $Met^{184}$ and $Met^{185}$ [4], and $Lys^{8}$ was restrained to $Asp^{130}$ [23]. The backbone atoms of the rUT receptor transmembrane domains were held in their positions during this step. The ligand and the extracellular and intracellular loops were free to move and interact. The U-II/rUT receptor complex was refined by several energy minimization steps until the maximum derivative was less than 0.1 kcal/mol. Molecular graphics figures were generated using Pymol [13].

## 3. Results

### 3.1. Binding properties of mutant receptors with cysteines in TMD6 and TMD7

To identify residues in TMD6 and TMD7 that face the binding-site pocket of the rUT receptor, we mutated 27 consecutive residues between $R256^{(6.32)}$ and $Q283^{(6.59)}$ of TMD6 and 26 consecutive residues between $A295^{(7.31)}$ and $Q283^{(7.57)}$ of TMD7 to cysteine, one at a time (Fig. 1). Each mutant receptor was transiently expressed in COS-7 cells. To assess the conservation of the overall conformation of these receptors after the substitutions, the pharmacological parameters of the equilibrium binding of the radiolabeled ligand $^{125}$I-U-II ($K_d$ and $B_{max}$) were determined (Tables 1 and 2). Most mutant receptors exhibited high binding affinity for $^{125}$I-U-II, similar to that of the wild-type UT receptor. TMD6 mutants $L267C^{(6.43)}$, $P274C^{(6.50)}$, $F275C^{(6.51)}$, $Q279C^{(6.55)}$, and $L281C^{(6.57)}$, and TMD7 mutants $N299C^{(7.35)}$, $P314C^{(7.50)}$, $L316C^{(7.52)}$, and $L319C^{(7.55)}$ did not demonstrate any detectable binding activity and were not used for the SCAM analyses.

### 3.2. Effect of extracellularly added MTSEA on the binding properties of TMD6 and TMD7 mutant receptors

To verify whether the reporter cysteines introduced into either TMD6 or TMD7 were oriented toward the binding pocket, cells expressing the UT mutant receptors were treated with 0.5–2 mM MTSEA for 3 min. We first verified whether the wild-type

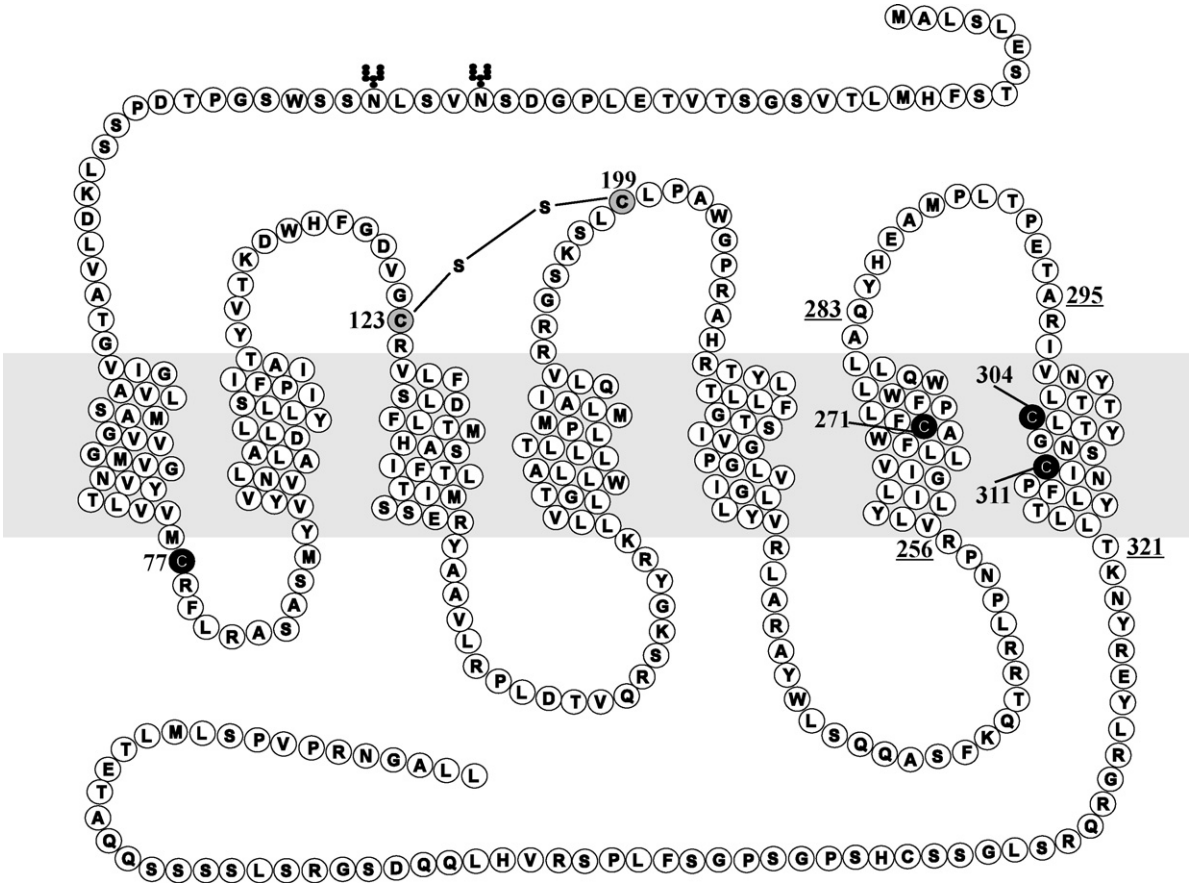


**Fig. 1.** Schematic representation of the rat UT receptor. The numbers indicate the positions of cysteines and other residues in the receptor. The grey closed circles represent cysteines that are thought to be linked via disulfide bridges, and the black closed circles represent cysteines whose side chains do not form a disulfide bridge. Mutated TMD6 residues are located between $Lys256^{(6.32)}$ and $Leu283^{(6.59)}$ inclusively. Mutated TMD7 residues are located between $Lys295^{(7.31)}$ and $Leu321^{(7.57)}$ inclusively. Putative Asn-glycosylation sites (N4, N176, N188) are indicated.

**Table 1**
Binding properties of U-II to cysteine-substituted rUT TMD6 mutant receptors.

| | $K_d$ (nM) | $B_{max}$ (pmol/mg protein) | $n$ |
|---|---|---|---|
| rUT | 3.1 ± 0.5 | 30.6 ± 7.4 | 6 |
| Q283C | 1.6 ± 1.4 | 21.9 ± 17.4 | 3 |
| A282C | 3.0 ± 0.3 | 23.5 ± 7.28 | 4 |
| L280C | 2.5 ± 1.2 | 2.5 ± 0.4 | 3 |
| W278C | 4.8 ± 0.4 | 15.3 ± 5.9 | 3 |
| L277C | 3.2 ± 0.4 | 21.8 ± 8.7 | 3 |
| W276C | 2.7 ± 0.8 | 2.51 ± 0.2 | 3 |
| L273C | 3.9 ± 1.5 | 20.8 ± 5.4 | 3 |
| F272C | 10.6 ± 3.0 | 15.9 ± 10.2 | 3 |
| A270C | 2.6 ± 0.4 | 17.0 ± 5.9 | 3 |
| W269C | 0.9 ± 0.2 | 5.5 ± 4.1 | 3 |
| F268C | 4.5 ± 1.0 | 0.6 ± 0.3 | 3 |
| L266C | 3.3 ± 0.4 | 28.4 ± 4.0 | 3 |
| V265C | 2.3 ± 0.8 | 15.5 ± 6.9 | 3 |
| I264C | 2.2 ± 0.3 | 17.6 ± 4.5 | 3 |
| G263C | 5.1 ± 2.2 | 23.0 ± 10.6 | 3 |
| L262C | 1.0 ± 0.4 | 4.7 ± 3.5 | 3 |
| I261C | 0.6 ± 0.3 | 5.2 ± 2.1 | 3 |
| L260C | 4.4 ± 1.1 | 29.9 ± 10.4 | 3 |
| Y259C | 3.4 ± 1.2 | 26.1 ± 4.8 | 3 |
| L258C | 3.1 ± 1.4 | 24.2 ± 3.7 | 3 |
| V257C | 3.0 ± 0.8 | 23.2 ± 8.6 | 3 |
| R256C | 3.3 ± 0.8 | 15.6 ± 10.5 | 3 |

Cells transfected with the appropriate receptor were assayed as described in Experimental Procedure. Binding affinities ($K_d$) and maximal binding capacities ($B_{max}$) are expressed as the means ± SD of values obtained in $n$ independent experiments performed in duplicate. Mutants L267C, P274C, F275C, Q279C, and L281C did not exhibit any detectable binding.

**Table 2**
Binding properties of U-II to cysteine-substituted rUT TMD7 mutant receptors.

| | $K_d$ (nM) | $B_{max}$ (pmol/mg protein) | $n$ |
|---|---|---|---|
| rUT | 3.1 ± 0.5 | 30.6 ± 7.4 | 6 |
| A295C | 7.0 ± 2.8 | 27.2 ± 3.0 | 3 |
| R296C | 5.3 ± 1.6 | 27.4 ± 18.2 | 3 |
| I297C | 5.5 ± 0.6 | 28.6 ± 4.2 | 3 |
| V298C | 4.2 ± 2.0 | 11.4 ± 9.7 | 3 |
| Y300C | 8.1 ± 5.2 | 43.8 ± 2.6 | 3 |
| L301C | 4.0 ± 1.1 | 37.8 ± 2.5 | 3 |
| T302C | 7.0 ± 2.4 | 34.4 ± 2.0 | 3 |
| T303C | 3.1 ± 0.9 | 25.6 ± 12.0 | 3 |
| L305C | 3.5 ± 0.5 | 21.3 ± 3.2 | 3 |
| T306C | 3.6 ± 0.4 | 48.3 ± 1.9 | 3 |
| Y307C | 6.1 ± 3.5 | 10.3 ± 4.3 | 3 |
| G308C | 2.2 ± 1.0 | 5.0 ± 4.9 | 3 |
| N309C | 1.4 ± 0.2 | 17.9 ± 0.7 | 3 |
| S310C | 4.5 ± 1.0 | 36.7 ± 9.9 | 3 |
| I312C | 4.8 ± 1.8 | 41.0 ± 9.3 | 3 |
| N313C | 1.9 ± 0.7 | 7.3 ± 5.5 | 3 |
| F315C | 3.9 ± 0.5 | 42.9 ± 3.1 | 3 |
| Y317C | 1.4 ± 0.2 | 12.4 ± 1.3 | 3 |
| T318C | 14.7 ± 2.2 | 28.2 ± 1.3 | 3 |
| L320C | 0.9 ± 0.2 | 16.6 ± 0.8 | 3 |
| T321C | 4.7 ± 1.1 | 26.3 ± 1.9 | 3 |

Cells transfected with the appropriate receptor were assayed as described in the Experimental Procedure. Binding affinities ($K_d$) and maximal binding capacities ($B_{max}$) are expressed as the means ± SD of values obtained in $n$ independent experiments performed in duplicate. Mutants N299C, N314C, L316C, and L319C did not exhibit any detectable binding.

UT receptor, which contains six endogenous cysteines (Fig. 1), was sensitive to MTSEA treatment and found that the various concentrations had very little effect (no more than a 10% reduction at high concentrations) on the binding properties of the wild-type UT receptor. This indicated that the endogenous cysteines made a relatively small contribution to the formation of the binding-site pocket of UT (Fig. 2A). For TMD6 mutants, Fig. 3 shows that treatment with 0.5 mM MTSEA strongly inhibited the U-II binding properties of mutant W278C$^{(6.54)}$ (binding inhibition of 56%). At 2 mM MTSEA, the binding properties of another mutant, F268C$^{(6.44)}$, was significantly inhibited (binding inhibition of 38%). For TMD7 mutants, Fig. 4 shows that treatment with 0.5 mM MTSEA strongly inhibited the U-II binding properties of three mutants: V298C$^{(7.34)}$ (binding inhibition of 45%), T302C$^{(7.38)}$ (binding inhibition of 73%), and T303C$^{(7.39)}$ (binding inhibition of 69%). The binding properties of all other TMD6 or TMD7 mutant receptors were not significantly affected by MTSEA treatment.

### 3.3. *Effect of extracellularly added MTSES on the binding properties of TMD6 and TMD7 mutant receptors*

Alkylation with MTS reagents may hamper the binding properties of the ligand in a mechanism involving steric hindrance, electrostatic repulsion, or a combination of both. As an alternative method to the use of a positively charged MTS compound (MTSEA), we treated each mutant receptor with the negatively charged alkylating agent MTSES for 3 min. MTSES had very little effect on the binding properties of the wild-type UT receptor (no more than a 5% reduction at high concentrations) (Fig. 2B). For TMD6, similar to the effects observed with MTSEA, treatment with 2 mM MTSES (Fig. 5) inhibited the binding properties of TMD6 mutants F268C$^{(6.44)}$ (binding inhibition of 23%) and W278C$^{(6.54)}$ (binding inhibition of 51%). Interestingly, MTSES treatment led to the significant inhibition in binding properties of an additional mutant receptor, namely A282C$^{(6.58)}$ (binding inhibition of 37%) not affected by MTSEA treatment.

For TMD7, mutants V298C$^{(7.34)}$ (binding inhibition of 45%), T302C$^{(7.38)}$ (binding inhibition of 70%) and T303C$^{(7.39)}$ (binding inhibition of 87%) were also robustly inhibited by treatment with 2 mM MTSES (Fig. 6). Again an additional mutant receptor not detected with MTSEA, Y300C$^{(7.36)}$, was significantly inhib-

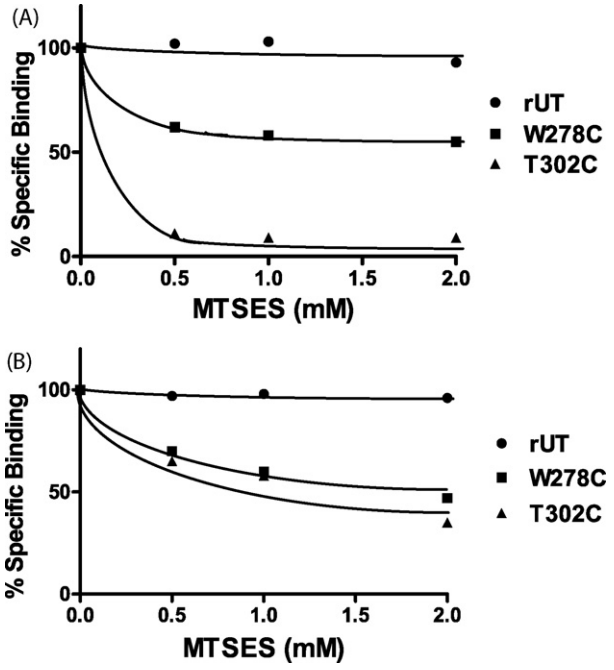


**Fig. 2.** Effect of MTS on the wild-type receptor and sensitive reporter cysteine-bearing mutant receptors. Intact COS-7 cells transiently expressing the rUT receptor, W278C, and T302C mutant receptors were incubated with MTSEA (A) or MTSES (B) in a final volume of 0.2 ml at room temperature for 3 min. The reaction was stopped by dilution in ice-cold PBS. The intact cells were then incubated with 0.05 nM $^{125}$I-U-II for 120 min at room temperature. The results are representative of three independent experiments.

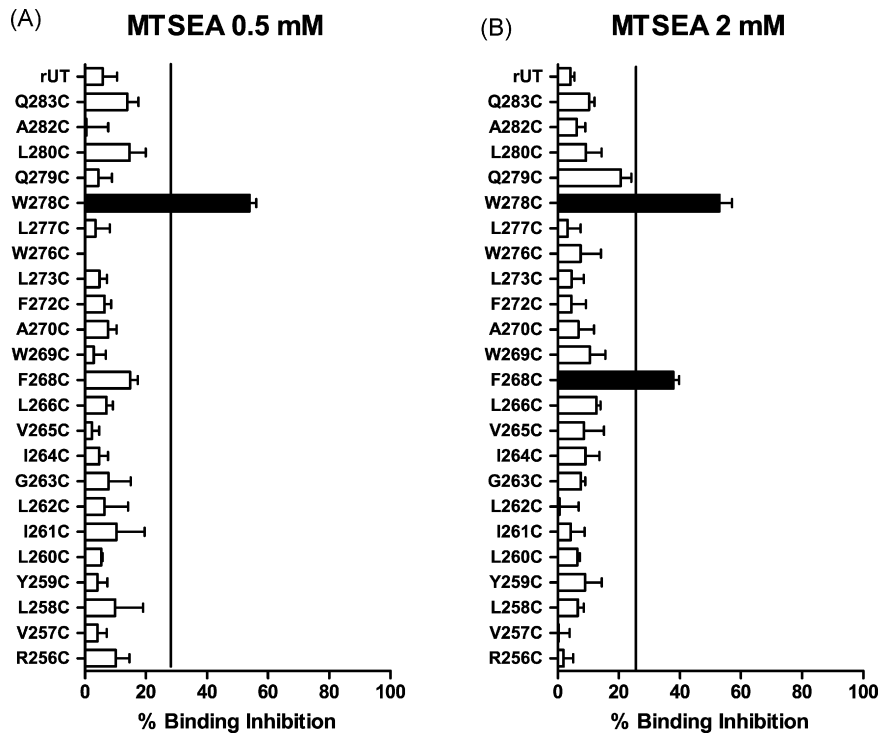


**Fig. 3.** Effects of MTSEA on UT receptor mutants bearing a reporter cysteine in TMD6. Intact COS-7 cells transiently expressing wild-type or TMD6 mutant rUT receptors were incubated for 3 min at room temperature with 0.5 mM MTSEA (A) or 2 mM MTSEA (B). The intact cells were then incubated for 120 min at room temperature with 0.05 nM $^{125}$I-U-II. The percentage of binding inhibition was calculated as indicated in Section 2. The vertical line represents an arbitrary threshold used to identify cysteine-sensitive mutants and was set at a value corresponding to binding inhibition 20% greater than that of the wild-type rUT receptor. The white bars indicate mutant receptors for which binding activities were not appreciably reduced compared to the wild-type receptor after MTSEA treatment. Black bars indicate mutant receptors for which binding activities were reduced after MTSEA treatment. Bars represent the mean ± SD of results from at least three independent experiments.

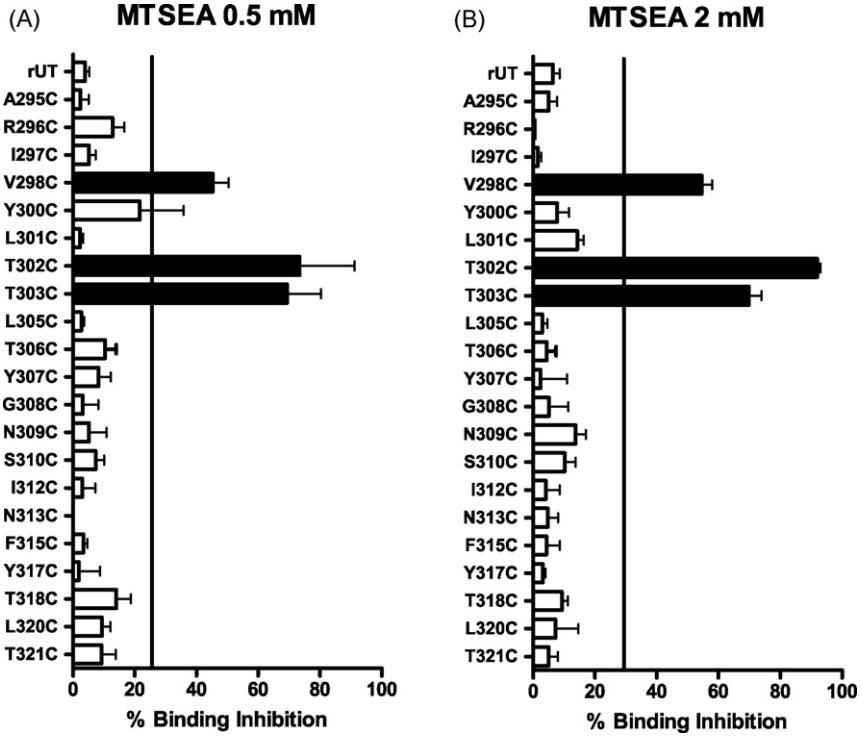


**Fig. 4.** Effect of MTSEA on UT receptor mutants bearing a reporter cysteine in TMD7. Intact COS-7 cells transiently expressing the wild-type or TMD7 mutant rUT receptors were incubated for 3 min at room temperature with 0.5 mM MTSEA (A) or 2 mM MTSEA (B). The intact cells were then incubated for 120 min at room temperature with 0.05 nM $^{125}$I-U-II. The percentage of binding inhibition was calculated as indicated in Section 2. The vertical line represents an arbitrary threshold used to identify cysteine-sensitive mutants. It was set at a value corresponding to binding inhibition 20% greater than that of the wild-type rUT receptor. The white bars indicate mutant receptors for which binding activities were not appreciably reduced compared to that of the wild-type receptor after MTSEA treatment. Black bars indicate mutant receptors for which binding activities were reduced after MTSEA treatment. Bars represent the mean ± SD of results from at least three independent experiments.

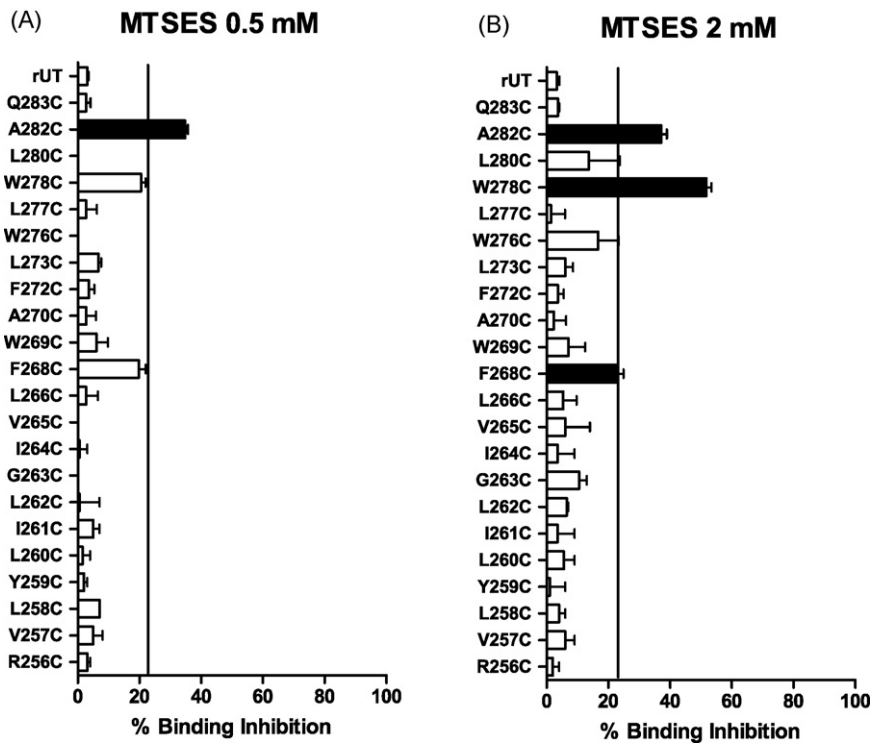


**Fig. 5.** Effects of MTSES on UT receptor mutants bearing a reporter cysteine in TMD6. Intact COS-7 cells transiently expressing wild-type or TMD6 mutant rUT receptors were incubated for 3 min at room temperature with freshly prepared 0.5 mM MTSES (A) or 2 mM MTSES (B). The intact cells were then incubated for 120 min at room temperature with 0.05 nM $^{125}$I-U-II. The percentage of binding inhibition was calculated as indicated in Section 2. The vertical line represents an arbitrary threshold used to identify cysteine-sensitive mutants and was set at a value corresponding to binding inhibition 20% greater than that of the wild-type rUT receptor. The white bars indicate mutant receptors for which binding activities were not appreciably reduced compared to the wild-type receptor after MTSES treatment. Black bars indicate mutant receptors for which binding activities were reduced after MTSES treatment. Bars represent the mean ± SD of results from at least three independent experiments.

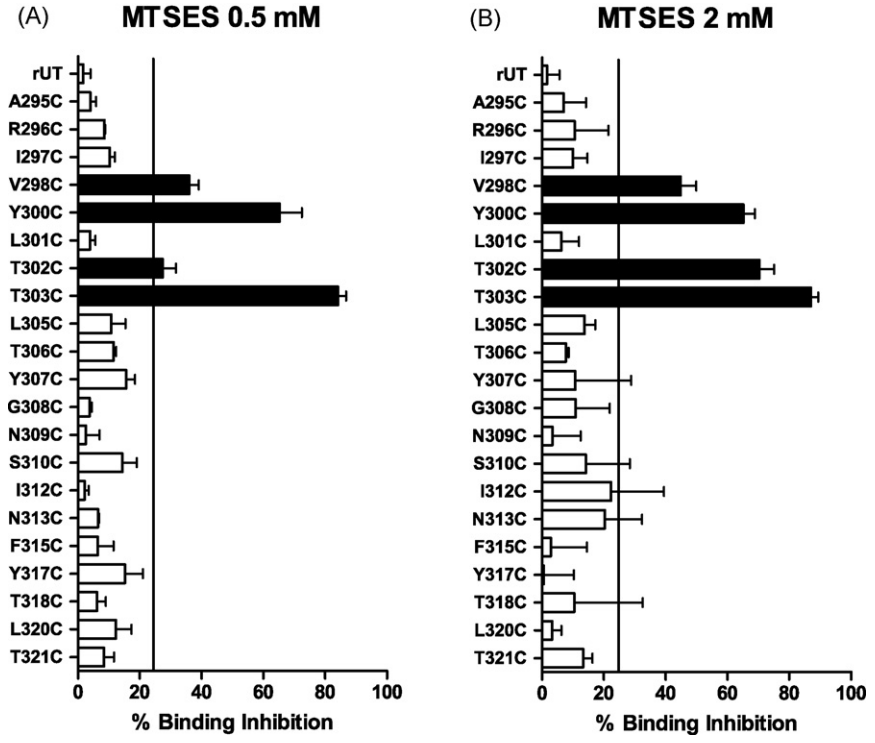


**Fig. 6.** Effect of MTSES on UT receptor mutants bearing a reporter cysteine in TMD7. Intact COS-7 cells transiently expressing wild-type or TMD7 mutant rUT receptors were incubated for 3 min at room temperature with 0.5 mM MTSES (A) or 2 mM MTSES (B). The intact cells were then incubated for 120 min at room temperature with 0.05 nM $^{125}$I-U-II. The percentage of binding inhibition was calculated as indicated in Section 2. The vertical line represents an arbitrary threshold used to identify cysteine-sensitive mutants. It was set at a value corresponding to binding inhibition 20% greater than that of the wild-type rUT receptor. The white bars indicate mutant receptors for which binding activities were not appreciably reduced compared to that of the wild-type receptor after MTSES treatment. Black bars indicate mutant receptors for which binding activities were reduced after MTSES treatment. Bars represent the mean ± SD of results from at least three independent experiments.

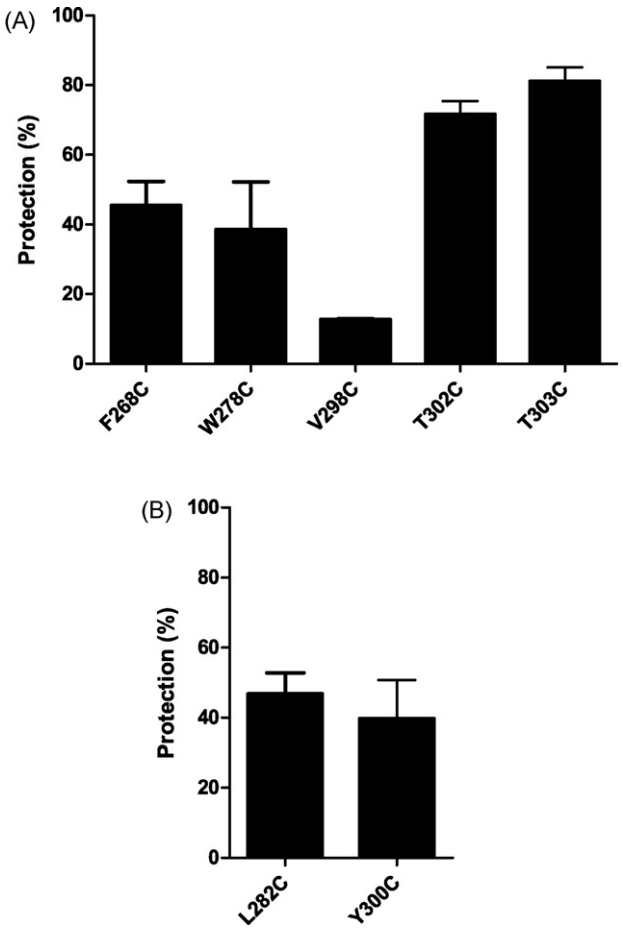


**Fig. 7.** UT protection of MTSEA-sensitive receptor mutants. Intact COS-7 cells transiently expressing the indicated MTSEA-sensitive (A) or MTSES-sensitive (B) mutant rUT receptors were pre-incubated for 1 h at 16 °C in the absence or presence of 100 nM U-II. The cells were then incubated for 3 min at 16 °C in the continued absence or presence of U-II with optimal MTSEA or MTSES concentrations to achieve maximal binding inhibition of each receptor. The MTS reagent concentrations were as follows: 2.0 mM for mutants L268C and W278C, 0.5 mM for mutants A282C, L298C, Y300C, T302C and T303C. The cells were then washed with ice-cold PBS and incubated for 3 h at 16 °C with 0.05 nM $^{125}$I-U-II. The degree of protection was calculated as described in Section 2. Bars represent the mean ± SD of results from at least three independent experiments.

ited (binding inhibition of 65%) when treated with 0.5 mM MTSES (as well as 2 mM MTSES). The binding properties of all other mutant receptors were not significantly affected by MTSES treatment.

### 3.4. Protection against MTS reagents by a pretreatment with U-II

To confirm that reporter cysteines accessible to MTSEA or MTSES were indeed located within the binding pocket of the UT receptor, mutants were incubated with the competitive ligand, U-II, prior to MTS treatment. Cells were then washed with an acid buffer to dissociate the bound ligand, and the receptors were assayed for binding with the radiolabeled competitive ligand. Pre-incubation with the ligand protected mutant receptors F268C$^{(6.44)}$, W278C$^{(6.54)}$, T302C$^{(7.38)}$, and T303C$^{(7.39)}$ from the inhibitory effect of MTSEA, with protection levels ranging from 38% to 81% (Fig. 7A), but only provided 13% protection for mutant V298C$^{(7.34)}$. Pre-incubation with U-II protected mutant receptors A282C$^{(6.58)}$ and T300C$^{(7.36)}$ from the inhibitory effect of MTSES, with protection levels of 47% and 40%, respectively (Fig. 7B). It should be noted that the pre-incubation with U-II also protected mutants F268C$^{(6.44)}$, W278C$^{(6.54)}$, V298C$^{(7.34)}$, and T302C$^{(7.38)}$, and T303C$^{(7.39)}$ from the effects of MTSES (data not shown).

## 4. Discussion

The rationale of this study, which relied on SCAM analyses, was to gain an insight into the orientation of TMD6 and TMD7 residues of the UT receptor by identifying residues accessible to MTS reagents within its binding-site pocket. Since water-accessible ionized thiolates react $10^9$ faster than un-ionized thiols [22], only water-accessible cysteines should be alkylated by MTS reagents. Ligand binding is likely hampered by MTS compounds via mechanisms involving steric hindrance, electrostatic repulsion, or indirect interaction. The tracer peptide used in our study was the full-length agonist of the wild-type UT receptor since we felt that it would enable us to identify determinants that might otherwise be missed with smaller peptide or non-peptide UT receptor ligands.

The rUT receptor has six endogenous cysteines, two of which are thought to be involved in the putative disulfide bridge linking ECL1 and ECL2. Of the four remaining endogenous cysteines, one is located in TMD6 (C271$^{(6.47)}$) and two are located in TMD7 (C304$^{(7.40)}$ and C311$^{(7.47)}$). The wild-type UT receptor is insensitive to both MTSEA and MTSES at concentrations up to 6 mM (Fig. 2 and data not shown). This suggests that endogenous cysteines are not alkylated by MTS reagents or that alkylation does not affect ligand binding properties. Our approach of adding the MTS reagent to whole adherent cells expressing the UT receptor essentially exposed only the extracellular, ligand-accessible side of the receptor.

Using MTSEA and MTSES, we identified three sensitive residues in TMD6, two at the top of the domain (W278$^{(6.54)}$ and A282$^{(6.58)}$) and one in the middle portion of the domain (F268$^{(6.44)}$). Residue A282$^{(6.58)}$ was sensitive to negatively charged MTSES but not to positively charged MTSEA. This would be due to an electrostatic repulsion effect caused by the proximity of a negatively charged determinant in the vicinity of A282$^{(6.58)}$, which would be located either in the receptor, thus affecting local receptor conformation, or in the ligand, thus affecting binding. We also demonstrated that L267C$^{(6.43)}$, P274C$^{(6.50)}$, F275C$^{(6.51)}$, Q279C$^{(6.55)}$, and L281C$^{(6.57)}$ lost their ability to bind U-II. Since position 6.50 is the structurally critical proline residue of TMD6, the loss of binding by the P274C$^{(6.50)}$ mutant was not surprising. Positions 6.51 and 6.55 are critical binding-site residues in a number of GPCRs [7,19,27,34].

We identified four sensitive residues (L298$^{(7.34)}$, Y300$^{(7.36)}$, T302$^{(7.38)}$, and T303$^{(7.39)}$) in TMD7 that are proximal to the extracellular side of the TMD. Unlike other receptors that we and others have studied using the SCAM approach, we were unable to detect sensitive residues deeper in TMD7 than T303$^{(7.39)}$ [3,17,35]. Y300$^{(7.36)}$ was sensitive to MTSES but not MTSEA, which again suggests that a negatively charged determinant is present in the vicinity of this residue. We also showed that N299C$^{(7.35)}$, P314C$^{(7.50)}$, L316C$^{(7.52)}$, and L319C$^{(7.55)}$ lost their ability to bind U-II. Residues P314$^{(7.50)}$ and L316$^{(7.52)}$ are part of the well-conserved NPxxY motif of TMD7 that is thought to participate in a network of interactions that either maintains the receptor in an inactive state or helps stabilize the active state [33]. With the exception of the L298C$^{(7.34)}$ mutant, the competitive U-II ligand protected all mutants tested in the protection assay, supporting the notion that these sensitive amino acids are located in the binding pocket. L298C$^{(7.34)}$ was poorly protected by U-II, suggesting that alkylation of this residue inhibits binding via a mechanism involving an indirect interaction with the receptor.

To assess the relative positions of the residues identified in the binding pocket of the rUT receptor, we modeled the U-II/rUT receptor complex by homology with the β2 adrenergic receptor crystal structure [7]. The complex was modeled using the distance

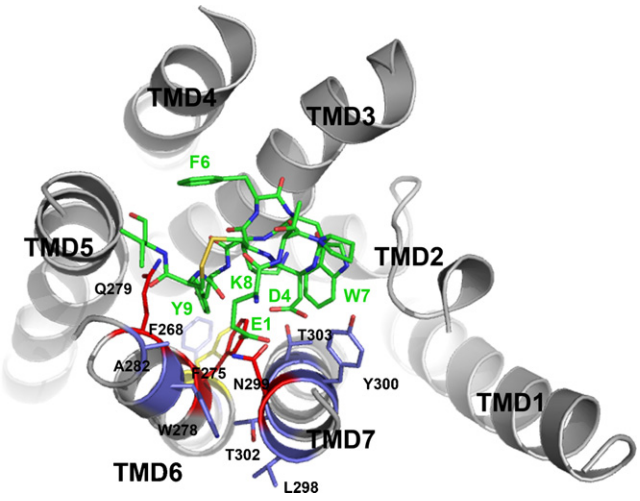


**Fig. 8.** Molecular model of rUT receptor. An extracellular view of the seven TMDs of the rUT receptor based on the model described for the β2 adrenergic receptor [7]. The water-accessible crevice forming the binding pocket is suggested to be located between TMDs 1, 2, 3, 5, 6, and 7. In the ground state, constraining intramolecular interactions help maintain the receptor in a basal state where functional coupling with the G-protein is kept to a minimum. The U-II ligand is shown in green. MTS positive residues F268$^{(6.44)}$, W278$^{(6.54)}$, A282$^{(6.58)}$, L298$^{(7.34)}$, Y300$^{(7.36)}$, T302$^{(7.38)}$, and T303$^{(7.39)}$ are indicated in blue. Residues F275$^{(6.51)}$, Q279$^{(6.55)}$, and N299$^{(7.35)}$, where cysteine substitution caused loss of binding, are indicated in red. The conserved 'toggle switch' residue F272$^{(6.48)}$ is shown in yellow.

restraints determined in previous photolabeling studies [4,18] to correctly position U-II in the receptor binding pocket (Fig. 8). When the complex was minimized with defined distance restraints, the structure of docked U-II had an RMSD (backbone atoms) value of 2.4 Å compared with the initial U-II structure, while the rUT receptor transmembrane domains had an RMSD (backbone atoms) value of 0.6 Å compared the initial model, indicating that the structures of both the ligand and the receptor had changed very little during the docking process. In our model, the residues making up the pharmacophore of U-II (W7, K8 and Y9) were well oriented in a binding pocket formed by the transmembrane domains of the rUT receptor.

The model in Fig. 8 shows that residue F268$^{(6.44)}$ is well positioned toward the interior of the transmembrane bundle and is deep inside the pocket relative to the other MTS-sensitive residues. In rhodopsin, the analogous F261$^{(6.44)}$ residue contacts the retinal ligand [27], whereas mutation of residue F282$^{(6.44)}$ of the β2 adrenergic receptor results in various degrees of constitutive activity [6], indicating that position 6.44 is also important for activation. SCAM analyses [25] and Methionine Proximity Assays [8] have shown that residue F249$^{(6.44)}$ is located in the binding pocket of the $AT_1$ receptor. This position in class A GPCRs F268$^{(6.44)}$ is located one helical turn below residue F272$^{(6.48)}$, the hypothesized 'rotamer toggle switch' in the CW/FLP motif [32]. F272$^{(6.48)}$ was not detected as an MTS sensitive residue using SCAM, but affinity of U-II towards the F272C$^{(6.48)}$ mutant was slightly reduced when compared to wild-type UT receptor (Table 1).

The model also reveals that residue W278$^{(6.54)}$ is proximal to the MTS-sensitive residues A282$^{(6.58)}$, V298$^{(7.34)}$, and T302$^{(7.38)}$. SCAM studies have shown that this position in the D2 receptor [17] and the μ, δ, and κ opioid receptors [36] is also sensitive to MTS. Our model also shows that A282$^{(6.58)}$ is positioned toward the helical bundle and is in close proximity to residues W278$^{(6.54)}$ and N299$^{(7.35)}$. Residues F275 and Q279 are located in the binding pocket, even though we were unable to obtain SCAM sensitivity due to the lack of binding of the F275C$^{(6.51)}$ and Q279C$^{(6.55)}$ mutant receptors to U-II. Residue F275$^{(6.51)}$ is in close proximity to the critical residues W7, K8, and Y9 of U-II. There is a similar interaction between position 6.51 and the ligand in rhodopsin and the β2 adrenergic receptor [7,27]. Residue Q279$^{(6.55)}$ is proximal to Y9 of U-II, and analogous interactions can be found in the β1 adrenergic and $A_{2A}$ adenosine receptors [19,34]. It is thus likely that residues F275C$^{(6.51)}$ and Q279C$^{(6.55)}$ are located in the binding pocket of the UT receptor.

As for the MTS-sensitive residues in TMD7, our model shows that MTSES-sensitive residue Y300$^{(7.36)}$ faces the binding pocket. This residue is located one helical turn above residue T303$^{(7.39)}$ and may be involved in π stacking or hydrogen bonding with W7 of U-II. Furthermore, residue T302$^{(7.38)}$ is oriented toward TMD6 and is in proximity to residues F275$^{(6.51)}$, W278$^{(6.54)}$, and V298$^{(7.34)}$. Studies on the D2 receptor using the SCAM approach [17] and on the $A_1$ adenosine receptor [12] have shown that this position faces the binding pocket of the respective receptors. The model also directs residue T303$^{(7.39)}$ toward the binding pocket and places it close to residues F275$^{(6.51)}$ and Y300$^{(7.36)}$. Residue T303$^{(7.39)}$ is in close proximity to the pharmacophoric residues W7 and K8 of U-II, which is in agreement with SCAM studies of the D2 [17], the $A_1$ adenosine, and the κ and δ opioid [35] receptors showing that position 7.39 faces the binding pocket of these GPCRs. Moreover, the crystal structure of the $A_{2A}$ adenosine receptor has revealed that I274$^{(7.39)}$ interacts directly with ZM241385, an $A_{2A}/A_{2B}$ antagonist [19]. While the N299C$^{(7.35)}$ mutant receptor was unable to bind U-II and could not be used for SCAM studies, the model shows N299$^{(7.35)}$ to be facing the helix bundle, enabling it to lie in close proximity to W278$^{(6.54)}$ and residues W7 and K9 of U-II. In both the β2 adrenergic and $A_{2A}$ crystal structures, this position interacts with the cognate ligands of the receptors [7,19].

It should be noted that several SCAM-positive residues, residues F268$^{(6.44)}$, W278$^{(6.54)}$ and T303$^{(7.39)}$, show $k_d$ values unchanged from the wild-type UT receptor. At first glance, this would suggest that introduction of cysteine residues at these positions does not disturb the structure of the receptor. Upon inspection of the molecular model, we note that the cysteine side-chains at these positions are within the binding site (Fig. 8) and therefore fully accessible for alkylation, thereby affecting the binding of the ligand. Hence, it is the alkylation with the MTS reagents and presence in the binding pocket, not the nature of the side chain, which would reduce binding.

Our results indicate that the V298C$^{(7.34)}$ mutant is MTSEA sensitive and that pre-incubating this mutant with U-II prior to the MTS treatment did not have a protective effect. In our model, even though V298$^{(7.34)}$ faces the exterior of the helix bundle, the residue is in close proximity to other MTSEA-sensitive residues such as W278$^{(6.54)}$ and T302$^{(7.38)}$. One explanation for the sensitivity of V298$^{(7.34)}$ to MTSEA is that it is involved in a network of interactions that are critical for receptor stability and ligand recognition. This network may involve other proximal MTS-sensitive residues such as W278$^{(6.54)}$, A282$^{(6.58)}$, T302$^{(7.38)}$, and N299$^{(7.35)}$ and could be destabilized following MTSEA or MTSES treatment of the V298C$^{(7.34)}$ mutant. Lastly, the binding inhibition observed for the A282C$^{(6.58)}$ and Y300C$^{(7.36)}$ following MTSES treatment may be due to charge repulsion between the negatively charged alkylated cysteines and the side chains of either E1 or D4 originating from the U-II ligand.

In conclusion, we identify specific residues in TMD6 and TMD7 that participate in the formation of the binding pocket of the UT receptor. Our results suggest that the UT receptor binding pocket shares many similarities with those of previously described class A GPCRs. The model generated from our results also indicates that residue W278$^{(6.54)}$ may be a focal point of interactions involving many of the residues identified in the present study. This network of interactions may be a distinctive feature of the UT receptor binding pocket.

## Acknowledgements

This work was supported by grants from the Canadian Institutes of Health Research and the Heart and Stroke Foundation of Canada. R.L. is a Chercheur National of the Fonds de la Recherche en Santé du Québec. E.E. is recipient of the J.C. Edwards Chair in Cardiovascular Research.

## References

[1] Akabas MH, Stauffer DA, Xu M, Karlin A. Acetylcholine receptor channel structure probed in cysteine-substitution mutants. Science 1992;258:307–10.
[2] Ames RS, Sarau HM, Chambers JK, Willette RN, Aiyar NV, Romanic AM, et al. Human urotensin-II is a potent vasoconstrictor and agonist for the orphan receptor GPR14. Nature 1999;401:282–6.
[3] Boucard AA, Roy M, Beaulieu ME, Lavigne P, Escher E, Guillemette G, et al. Constitutive activation of the angiotensin II type 1 receptor alters the spatial proximity of transmembrane 7 to the ligand-binding pocket. J Biol Chem 2003;278:36628–36.
[4] Boucard AA, Sauve SS, Guillemette G, Escher E, Leduc R. Photolabelling the rat urotensin II/GPR14 receptor identifies a ligand-binding site in the fourth transmembrane domain. Biochem J 2003;370:829–38.
[5] Carotenuto A, Grieco P, Campiglia P, Novellino E, Rovero P. Unraveling the active conformation of urotensin II. J Med Chem 2004;47:1652–61.
[6] Chen S, Lin F, Xu M, Riek RP, Novotny J, Graham RM. Mutation of a single TMVI residue, Phe(282), in the beta(2)-adrenergic receptor results in structurally distinct activated receptor conformations. Biochemistry 2002;41:6045–53.
[7] Cherezov V, Rosenbaum DM, Hanson MA, Rasmussen SG, Thian FS, Kobilka TS, et al. High-resolution crystal structure of an engineered human beta2-adrenergic G protein-coupled receptor. Science 2007;318:1258–65.
[8] Clement M, Martin SS, Beaulieu ME, Chamberland C, Lavigne P, Leduc R, et al. Determining the environment of the ligand binding pocket of the human angiotensin II type I (hAT1) receptor using the methionine proximity assay. J Biol Chem 2005;280:27121–9.
[9] Coulouarn Y, Jegou S, Tostivint H, Vaudry H, Lihrmann I. Cloning, sequence analysis and tissue distribution of the mouse and rat urotensin II precursors. FEBS Lett 1999;457:28–32.
[10] Coulouarn Y, Lihrmann I, Jegou S, Anouar Y, Tostivint H, Beauvillain JC, et al. Cloning of the cDNA encoding the urotensin II precursor in frog and human reveals intense expression of the urotensin II gene in motoneurons of the spinal cord. Proc Natl Acad Sci USA 1998;95:15803–8.
[11] Dauber-Osguthorpe P, Roberts VA, Osguthorpe DJ, Wolff J, Genest M, Hagler AT. Structure and energetics of ligand binding to proteins: *Escherichia coli* dihydrofolate reductase-trimethoprim, a drug-receptor system. Proteins 1988;4:31–47.
[12] Dawson ES, Wells JN. Determination of amino acid residues that are accessible from the ligand binding crevice in the seventh transmembrane-spanning region of the human A(1) adenosine receptor. Mol Pharmacol 2001;59:1187–95.
[13] DeLano WL. The PyMOL molecular graphics system. San Carlos, CA: Delano Scientific; 2002.
[14] Desai N, Sajjad J, Frishman WH. Urotensin II: a new pharmacologic target in the treatment of cardiovascular disease. Cardiol Rev 2008;16:142–53.
[15] Douglas SA. Human urotensin-II as a novel cardiovascular target: 'heart' of the matter or simply a fishy 'tail'? Curr Opin Pharmacol 2003;3:159–67.
[16] Fraker PJ, Speck Jr JC. Protein and cell membrane iodinations with a sparingly soluble chloroamide 1,3,4,6-tetrachloro-3a,6a-diphrenylglycoluril. Biochem Biophys Res Commun 1978;80:849–57.
[17] Fu D, Ballesteros JA, Weinstein H, Chen J, Javitch JA. Residues in the seventh membrane-spanning segment of the dopamine D2 receptor accessible in the binding-site crevice. Biochemistry 1996;35:11278–85.
[18] Holleran BJ, Beaulieu ME, Proulx CD, Lavigne P, Escher E, Leduc R. Photolabelling the urotensin II receptor reveals distinct agonist- and partial-agonist-binding sites. Biochem J 2007;402:51–61.
[19] Jaakola VP, Griffith MT, Hanson MA, Cherezov V, Chien EY, Lane JR, et al. The 2.6 Angstrom crystal structure of a human A2A adenosine receptor bound to an antagonist. Science 2008.
[20] Javitch JA, Ballesteros JA, Weinstein H, Chen J. A cluster of aromatic residues in the sixth membrane-spanning segment of the dopamine D2 receptor is accessible in the binding-site crevice. Biochemistry 1998;37:998–1006.
[21] Javitch JA, Li X, Kaback J, Karlin A. A cysteine residue in the third membrane-spanning segment of the human D2 dopamine receptor is exposed in the binding-site crevice. Proc Natl Acad Sci USA 1994;91:10355–9.
[22] Javitch JA, Shi L, Liapakis G. Use of the substituted cysteine accessibility method to study the structure and function of G protein-coupled receptors. Methods Enzymol 2002;343:137–56.
[23] Kinney WA, Almond Jr HR, Qi J, Smith CE, Santulli RJ, de Garavilla L, et al. Structure-function analysis of urotensin II and its use in the construction of a ligand-receptor working model. Angew Chem Int Ed Engl 2002;41:2940–4.
[24] Martin SS, Boucard AA, Clement M, Escher E, Leduc R, Guillemette G. Analysis of the third transmembrane domain of the human type 1 angiotensin II receptor by cysteine scanning mutagenesis. J Biol Chem 2004;279:51415–23.
[25] Martin SS, Holleran BJ, Escher E, Guillemette G, Leduc R. Activation of the angiotensin II type 1 receptor leads to movement of the sixth transmembrane domain: analysis by the substituted cysteine accessibility method. Mol Pharmacol 2007;72:182–90.
[26] Ong KL, Lam KS, Cheung BM. Urotensin II: its function in health and its role in disease. Cardiovasc Drugs Ther 2005;19:65–75.
[27] Palczewski K, Kumasaka T, Hori T, Behnke CA, Motoshima H, Fox BA, et al. Crystal structure of rhodopsin: A G protein-coupled receptor. Science 2000;289:739–45.
[28] Papadopoulos P, Bousette N, Giaid A. Urotensin-II and cardiovascular remodeling. Peptides 2008;29:764–9.
[29] Park JH, Scheerer P, Hofmann KP, Choe HW, Ernst OP. Crystal structure of the ligand-free G-protein-coupled receptor opsin. Nature 2008;454:183–7.
[30] Pearson D, Shively JE, Clark BR, Geschwind II, Barkley M, Nishioka RS, et al. Urotensin II: a somatostatin-like peptide in the caudal neurosecretory system of fishes. Proc Natl Acad Sci USA 1980;77:5021–4.
[31] Proulx CD, Holleran BJ, Lavigne P, Escher E, Guillemette G, Leduc R. Biological properties and functional determinants of the urotensin II receptor. Peptides 2008;29:691–9.
[32] Schwartz TW, Frimurer TM, Holst B, Rosenkilde MM, Elling CE. Molecular mechanism of 7TM receptor activation—a global toggle switch model. Annu Rev Pharmacol Toxicol 2006;46:481–519.
[33] Smit MJ, Vischer HF, Bakker RA, Jongejan A, Timmerman H, Pardo L, et al. Pharmacogenomic and structural analysis of constitutive g protein-coupled receptor activity. Annu Rev Pharmacol Toxicol 2007;47:53–87.
[34] Warne T, Serrano-Vega MJ, Baker JG, Moukhametzianov R, Edwards PC, Henderson R, et al. Structure of a beta1-adrenergic G-protein-coupled receptor. Nature 2008;454:486–91.
[35] Xu W, Campillo M, Pardo L, Kim de Riel J, Liu-Chen LY. The seventh transmembrane domains of the delta and kappa opioid receptors have different accessibility patterns and interhelical interactions. Biochemistry 2005;44:16014–25.
[36] Xu W, Li J, Chen C, Huang P, Weinstein H, Javitch JA, et al. Comparison of the amino acid residues in the sixth transmembrane domains accessible in the binding-site crevices of mu, delta, and kappa opioid receptors. Biochemistry 2001;40:8018–29.